Site-Directed Mutagenesis of PsaA Residue W693 Affects Phylloquinone Binding and Function in the Photosystem I Reaction Center of *Chlamydomonas reinhardtii*†

Saul Purton,‡ David R. Stevens,‡ Irine P. Muhiuddin,‡ Michael C. W. Evans,‡ Susan Carter,‡ Stephen E. J. Rigby,§ and Peter Heathcote*,§

Department of Biology, University College London, University of London, Gower Street, London WC1E 6BT, U.K., and School of Biological Sciences, Queen Mary and Westfield College, University of London, Mile End Road, London E1 4NS, U.K.

Received August 16, 2000; Revised Manuscript Received November 13, 2000

ABSTRACT: To investigate the environment of the phylloquinone secondary electron acceptor A_1 within the photosystem I reaction center, we have carried out site-directed mutagenesis of two tryptophan residues (W693 and W702) in the PsaA subunit of *Chlamydomonas reinhardtii*. One of these conserved tryptophans (W693) is predicted to be close to the phylloquinone and has been implicated in the interaction of A_1 with an aromatic residue through $\pi-\pi$ stacking. We find that replacement of W702 with either histidine or leucine has no effect on the electronic structure of $A_1^{\bullet-}$ or on forward electron transfer from $A_1^{\bullet-}$ to the iron−sulfur center F_x. In contrast, the same mutations of W693 alter the electronic structure of the photoaccumulated $A_1^{\bullet-}$ and slow forward electron transfer as measured by the decay of the electron spin-polarized signal arising from the $P700^{\bullet+}/A_1^{\bullet-}$ radical pair. These results provide support for the hypothesis that W693 has a role in poising the redox potential of $A_1/A_1^{\bullet-}$ so it can reduce F_x, and they indirectly provide evidence for electron transfer along the PsaA-side branch of cofactors in PSI.

The photosystem I (PSI)[1] reaction center is a plastocyanin-ferredoxin oxidoreductase (see refs *1* and *2* for recent reviews). Light energy initiates electron transfer from a primary electron donor P700, which is a dimer of chlorophyll *a* molecules. The primary electron acceptor A_o is a chlorophyll *a* monomer, which then donates electrons to a phylloquinone (vitamin K_1) secondary electron acceptor A_1. Subsequently electrons are transferred to a bound [4Fe-4S] center, F_x, and then on to two further bound [4Fe-4S] centers called F_A and F_B. The PSI reaction center contains two major proteins PsaA and PsaB (*3*), which show extensive sequence homology, and form a heterodimeric complex binding P700, A_o, A_1, and F_x. The structure of PSI has been solved to 4 Å (*4*) and demonstrates that the reaction center has apparent C_2 symmetry with two possible routes of electron transfer from P700 to F_x via two alternative accessory chlorophylls and two alternative A_o acceptors. There are also two phylloquinone molecules in PSI (*5*) that have recently been located within the structure (*6*), but only one of these is required for forward electron transfer to the FeS electron acceptors (*7*). The F_A and F_B centers are bound by a small extrinsic protein PsaC (*8*, *9*), and the electron acceptor complex involves two additional small extrinsic proteins PsaD and PsaE (*10*, *11*). The complete PSI complex involves a total of at least 11 polypeptides and binds approximately 100 chlorophyll molecules. In photosynthetic eukaryotes the genes for PsaA, PsaB, PsaC, and several other small subunits are located on the chloroplast genome. The remaining subunits, including PsaD and PsaE, are nuclear encoded (*2*).

Although the role of phylloquinone in forward electron transfer from A_o to F_x has been demonstrated (*12*−*14*), the mechanism by which it is able to do so remains unresolved. The phylloquinone/phyllosemiquinone ($A_1/A_1^{\bullet-}$) redox couple in PSI has to function at a relatively low redox potential in order to participate in efficient electron transfer from A_o (the E_M of chlorophyll *a* in vitro is ∼900 mV; *15*) to F_x with an estimated E_M of −730mV (*16*). The PSI polypeptide binding this redox couple is presumed to engineer the E_M of $A_1/A_1^{\bullet-}$ so it can function in forward transfer, but the available crystal structure of PSI (*4*, *6*) is not of sufficient resolution to reveal the immediate environment of the two phylloquinones or indeed to model the location of amino acid residues within the structure.

The electronic structure of the phyllosemiquinone $A_1^{\bullet-}$ and the influence of the PSI polypeptides on that electronic structure and thus the redox potential of $A_1/A_1^{\bullet-}$ have been studied by paramagnetic resonance techniques, most notably by electron nuclear double resonance (ENDOR) and electron spin−echo envelope modulation (ESEEM). An electron paramagnetic resonance (EPR) signal has been assigned to $A_1^{\bullet-}$ by biosynthetic deuteration (*17*), which allowed sub-

† This work was supported by grants from the U.K. Biotechnology and Biological Sciences Research Council (BBSRC) (CO0350 and 7809) and a European Union TMR program (Contract FMRX-CT98-0214).

* To whom correspondence should be addressed. Phone: 44-20-7882-3019. E-mail: p.heathcote@qmw.ac.uk.

‡ University College London.

§ Queen Mary and Westfield College.

[1] Abbreviations: ECL, enhanced chemiluminescence; E_M, oxidation−reduction midpoint potential; ENDOR, electron nuclear double resonance; EPR, electron paramagnetic resonance; ESEEM, electron spin−echo envelope modulation: ESP, electron spin polarized; HRP, horseradish peroxidase; PAR, photosynthetically active radiance; PCR, polymerase chain reaction; PSI, photosystem I; P700, primary electron donor of photosystem I; A_o, chlorophyll primary electron acceptor in photosystem I; A_1, phylloquinone secondary electron acceptor in photosystem I; F_A, F_B, and F_x, [4Fe-4S] centers of photosystem I; PhQ, phylloquinone; hfcs, hyperfine couplings; RC, reaction center.

10.1021/bi0019489 CCC: $20.00
Published on Web 01/25/2001

sequent ENDOR (*18*, *19*) and ESEEM (*20*) studies. The ENDOR studies indicated relatively strong hydrogen bonds to both carbonyl oxygens from the protein and an increase in the 2-methyl and β-methylene hyperfine couplings (hfcs) relative to those observed for the phyllosemiquinone in vitro (*18*). However, studies of the electron spin-polarized (ESP) signal arising from the $P700^{\bullet+}/A_1^{\bullet-}$ radical pair (*21*) suggest weak or asymmetric hydrogen bonding, which would at least partially account for the low redox potential of $A_1/A_1^{\bullet-}$. Kamlowski *et al.* (*22*) reviewed the data available from paramagnetic resonance studies of the phylloquinone binding site in PSI and pointed out that the *g*-anisotropy of the semiquinone radical, and in particular the shift of the g_{xx} component of the *g*-tensor from the free electron value, is a qualitative measure of the interaction of the quinone with its environment. Measurement of the $g_{xx} - g_e$ at 95GHz (W band) (*21*) and at 283GHz (*23*) show that the $\Delta g_{xx} - g_e$ for $A_1^{\bullet-}$ is much larger than that for the strongly hydrogen bonded $Q_A^{\bullet-}$ in bacterial reaction centers. This is taken to indicate that the quinone acceptor in PSI experiences weaker H-bonding and/or stronger $\pi-\pi$ interaction with the protein environment in contrast to bacterial reaction centers. The ESEEM studies (*20*) indicated that tryptophan and histidine residues are very close to $A_1^{\bullet-}$, giving rise to the suggestion that $\pi-\pi$ stacking of the phylloquinone with an aromatic residue such as tryptophan could be the cause of the low redox potential. Studies of the orientation of $A_1^{\bullet-}$ relative to $P700^{\bullet+}$ (*23*) and determination of the distance between $P700^{\bullet+}$ and F_x by relaxation (*24*) and $P700^{\bullet+}$ and $A_1^{\bullet-}$ by ESEEM techniques (*25*), enabled the approximate location of the phylloquinone within the 4 Å structure (*22*). Modeling of the phylloquinone position and the residues predicted to be in that region from the structure and amino acid sequence indicated that a tryptophan residue (W697 in *Synechococcus elongatus*) of a conserved Tyr-Trp pair located at the start of helix *n* and *n*′ of PSI could be close to the phylloquinone (*22*). It is not known whether one or both of the two possible branches of electron transfer is active, and therefore whether one or both phylloquinones is active in electron transfer. However, ENDOR studies of mutants of the residues binding P700 (*26*) have suggested that the chlorophyll on PsaB carries most of the electron spin density in the cation $P700^{\bullet+}$. Therefore, by analogy with the reaction center of purple photosynthetic bacteria, it has been suggested that PsaB contains the active branch of electron transfer (*26*). The subsequent localization of the phylloquinones within the structure (*6*) was essentially in agreement with the earlier location predicted by ESEEM and relaxation techniques and modeling (*22*, *24*, *25*).

We have carried out site-directed mutagenesis of the tryptophan residue (W693) in the PsaA subunit of PSI in *C. reinhardtii* equivalent to the residue predicted to be close to phylloquinone in PSI from *S. elongatus* (*22*), together with modification of another tryptophan residue (W702) close to the putative phylloquinone binding region. The mutants all assemble functional PSI reaction centers and contain the minor subunits PsaD and PsaF. The ability of mutants to grow photoautotrophically was assessed by spot tests, and the presence of phylloquinone monitored by photoacccumulation of the phyllosemiquinone and EPR spectroscopy. More detailed information on the electronic structure and binding pocket of the phyllosemiquinone was provided by proton

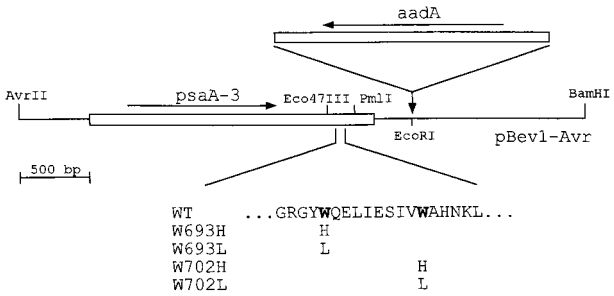

FIGURE 1: Site-directed mutagenesis of W693 and W702 in Psa A. Plasmid pBev1-Avr contains an *Avr*II−*Bam*HI fragment of the *C. reinhardtii* chloroplast genome encoding exon 3 of the Psa A gene together with the spectinomycin resistance cassette, *aadA* (*30*), inserted downstream of the gene. DNA changes to the coding region of *psaA-3* were made to replace tryptophan with that of either histidine or leucine as indicated.

ENDOR spectroscopy of the photoaccumulated phyllosemiquinone. The function of the phylloquinone in forward electron transfer was monitored by the decay of the ESP signal arising from the $P700^{\bullet+}/A_1^{\bullet-}$ radical pair (*12*). The results obtained provide support for the hypothesis that this tryptophan residue has a role in poising the redox potential of $A_1/A_1^{\bullet-}$ so that it can reduce F_x, and they indirectly provide evidence for electron transfer along the PsaA-side branch of cofactors in PSI.

MATERIALS AND METHODS

Plasmid Construction. The *recA Escherichia coli* strain DH5α was used in all recombinant DNA work. Plasmids for site-directed mutagenesis of *psaA-3* were derived from plasmid pBev1-Avr that contains the whole of *psaA-3* together with the *aadA* cassette used for selection of chloroplast transformants (*28*) (see Figure 1). Site-directed changes to the tryptophan codons were achieved using a two-step PCR strategy. (Details of the oligonucleotides used and an explanation of the PCR strategy can be found at http://www.ucl.ac.uk/biology/prg.htm.) For each mutation, a novel restriction enzyme site was introduced by making, where necessary, silent mutations in adjacent codons: W693H and W693L mutations introduce an *Eco*RV site, W702H introduces an *Sph*I site, and W702L introduces an *Nhe*I site. In each case, the final PCR product was digested with *Eco*47III and *Pml*I to generate a 232-bp fragment carrying the modified region of *psaA-3*. This was cloned into the corresponding sites in pBev1-Avr thereby replacing the wild-type sequence. Each construct was checked by restriction analysis and sequencing of the 232-bp region.

Chloroplast Transformation. The *C. reinhardtii* strain used as a recipient for transformation was wild-type mt+ (CC-1021) obtained from the Chlamydomonas Culture Collection (Duke University). The strain was cultured on Tris−acetate−phosphate (TAP) medium (*29*). Biolistic transformation of the chloroplast genome was carried out essentially as described by Goldschmidt-Clermont (*30*) using a Bio-Rad PDS1000/He biolistic device. For each bombardment, a lawn of recipient cells was prepared as follows: A 20-mL culture at approximately 4×10^6 cells/mL was harvested by brief centrifugation and resuspended in 0.5 mL of TAP medium. A total of 3 mL of molten TAP−0.5% agar was added, and the cells were plated to TAP−2% agar plates supplemented

with spectinomycin at 100 μg/mL, creating a lawn of approximately 8×10^7 target cells. Gold particles of 1.0 μm diameter were coated with 1 μg of plasmid DNA according to the manufacturer's protocol. The plates were bombarded with the DNA-coated gold using rupture disks with a burst pressure of 1100 psi. Plates were incubated in dim light [<1 μeinstein m^{-2} (s of PAR)$^{-1}$] at 25 °C. Spectinomycin-resistant colonies appeared after 2−3 weeks and were taken through three rounds of single-colony isolations to obtain homoplasmic transformants. Homoplasmicity was confirmed by Southern blot analysis of genomic DNA extracted from wild-type and transformant cells (*31*).

Growth of Mutants. Strains were grown in liquid TAP medium at 25 °C in darkness, since a PSI-minus mutant PsaA:C575D used as a control (see Results) was very light sensitive**.** Heterotrophic and phototrophic growth under both aerobic and anaerobic conditions were tested by spotting 5 μL of log-phase culture on TAP or high salt minimum (HSM) agar plates and growing under moderate light [45 μeinstein m^{-2} (s of PAR)$^{-1}$] (*29*). Anaerobiosis was achieved by placing plates in BBL GasPak bags (Becton Dickinson & Co.). These bags utilize iron powder and calcium carbonate to produce an anaerobic CO_2-enriched environment.

Western Analysis of PSI Assembly and Polypeptide Composition. To quantify the level of expression and polypeptide composition of PSI in mutants, Western analysis was carried out using whole cell extracts. Cells were grown in darkness to 3×10^6 cells/mL, pelleted, and resuspended in 0.8 M Tris HCl, pH 8.4; 0.2 M sorbitol; 1% 2-mecaptoethanol; and 1% SDS to 6×10^7 cell/mL. The 100-μL samples were boiled for 1 min, separated on a 15% SDS−polyacrylamide gel, and electroblotted to ECL nitrocellulose membrane (Amersham). Binding of antibodies was detected using the ECL detection system as supplied by Amersham. Primary antibodies to PsaD and PsaF were obtained from D. A. Bryant (*10*) and J.-D. Rochaix (*32*), respectively**,** and anti-PsaA antibodies were a gift from K. Redding (University of Alabama).

Biochemical Analysis. Cells were harvested from large-scale (10-L) cultures using a Millipore Pelicon filter system. The chloroplast membrane fraction was prepared by the procedure described by Diner and Wollman (*33*). The membranes were washed to remove excess sucrose and suspended in 20 mM Tris-HCl containing 100 mM NaCl. An enriched photosystem I preparation was made by treatment with digitonin following the procedure of Boardman (*34*) except that 1% digitonin was used. β-D-Maltoside PSI preparations were prepared as described by Fisher et al. (*35*).

CW and kinetic EPR measurements were made on digitonin PSI preparations at concentrations of 2−6 mg of chlorophyll/mL. For kinetic measurements, samples in standard 3-mm quartz EPR tubes were reduced either with sodium ascorbate (10 mM) or β-mercaptoethanol (1 mM) for 30 min in the dark prior to freezing in the dark in liquid nitrogen. Samples were stored in liquid nitrogen in the dark. To photoaccumulate $A_1^{\bullet-}$, the samples in standard EPR tubes were reduced for 30 min in the dark with sodium dithionite prior to freezing in liquid nitrogen. The $A_1^{\bullet-}$ was then photoaccumulated by 205 K illumination as described previously at pH 8 (*36*, *17*) and pH 10 (*23*).

Paramagnetic Resonance Spectroscopy (*CW EPR, Pulsed EPR, and ENDOR*). CW EPR spectra were recorded on a JEOL RE1X spectrometer fitted with an Oxford Instruments ESR9 liquid helium cryostat.

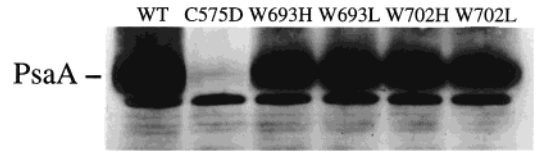

FIGURE 2: Western analysis of PSI assembly in the mutants. The wild-type strain, the four tryptophan mutants, and a site-directed mutant (PsaA:C575D) that fails to accumulate PSI were all grown in darkness in acetate-containing medium to mid-log phase. For each strain, total cell protein from 6×10^6 cells was analyzed by Western blotting using antibodies to PsaA. These antibodies also recognize a lower molecular weight protein unrelated to PSI.

Kinetic pulsed EPR spectra and kinetics were measured as described previously (*12*) using a Bruker ESP380 X-band spectrometer with a variable Q dielectric resonator (Bruker model 1052 DLQ-H 8907) fitted with an Oxford Instruments CF935 cryostat cooled with liquid nitrogen. Actinic illumination was supplied by a Nd:YAG laser (Spectra Physics DCR-11) with 10-ns pulse duration. The decay of the spin-polarized "out of phase" (*37*) signal reflecting the decay of the $P700^{\bullet+}/A_1^{\bullet-}$ radical pair was followed at 100 K to determine the rate of the back reaction between the two radicals. At this temperature, PSI reaction centers show one of two electron-transfer processes (*38*). In some centers, irreversible electron transfer to the $F_{A/B}$ centers is observed. In some centers, the electron is transferred from P700 to A_1 but does not go forward, the radical pair decaying by back reaction to P700. We have used this decay rate as an indicator of structural integrity of the P700/A_1 region of the reaction center.

At room temperature, the decay of the spin-polarized signal reflects the reoxidation of $A_1^{\bullet-}$ by F_x (*12*). However, it is extremely difficult to make these measurements at room temperature as only very small amounts of liquid water can be used in the spectrometer as the water absorbs microwaves preventing operation of the spectrometer. This means only very small samples can be used, and this makes it difficult, with the low amounts of PSI sometimes encountered in mutant strains of *C. reinhardtii*, to make room temperature measurements. However, this difficulty can be overcome if the sample can be frozen. Schlodder et al. (*38*) have shown that PSI forward electron transfer proceeds normally at temperatures down to 240 K, although it proceeds at a slower rate at lower temperatures. We have previously taken advantage of this to measure electron transfer from $A_1^{\bullet-}$ to F_x in preparations of *C. reinhardtii* at 260 K (*39*). ENDOR spectra were obtained at X-band using a Bruker ESP300 spectrometer as described by Rigby et al. (*40*, *41*).

RESULTS

Western Analysis of Amounts of PSI Assembled in Whole Cell Extracts of Mutants and of PSI Preparations for PsaD and PsaF Content. Western blotting of whole cell extracts from the wild-type strain and the mutants using antibodies to PsaA demonstrated that the PsaA protein accumulates to approximately 50% of wild-type levels in the W702 and W693 mutants (Figure 2). This is in contrast to a mutation (PsaA:C575D) that completely disrupts PSI assembly (*28*) where PsaA is barely detectable due to accelerated turnover

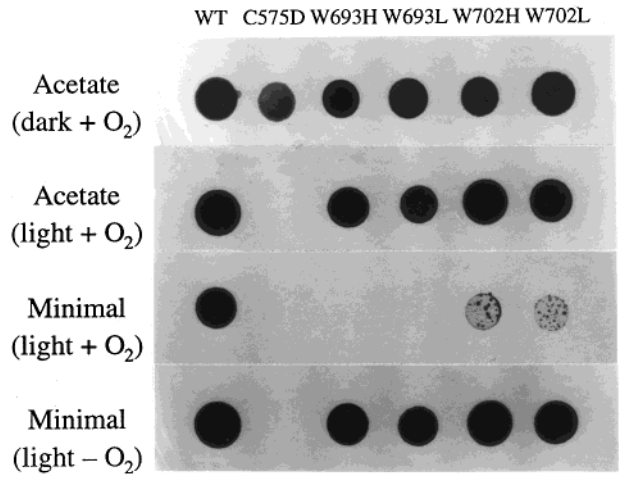

FIGURE 3: Growth properties of the mutants. Liquid cultures of the wild-type strain, the PSI-minus mutant C575D, and the four tryptophan mutants were prepared by growing in TAP medium in the dark and then spotted onto solid media. Acetate indicates TAP medium and supports heterotrophic growth, whereas minimal medium will only support phototrophic growth. Colonies were allowed to develop in darkness or 50 μeinstein m^{-2} s^{-1} light and in the presence or absence of oxygen as indicated.

of the unassembled protein. The data therefore indicate that the PSI complex assembles in each of the tryptophan mutants, albeit to a reduced level. Further Western analysis using antibodies to PsaD and PsaF show that these subunits accumulate in each of the four mutants and the wild type to approximately the same levels relative to the amount of PsaA (data not shown), indicating that the subunit composition of the PSI complex is not affected by the mutation of the tryptophan residues. In addition to demonstrating that PSI is assembling properly in the mutants, this also indicates that any changes seen in phyllosemiquinone photoaccumulation are due to the substitution of residues in PsaA rather than indirect effects caused by the loss of smaller subunits, as reported in the case of deletion of PsaE and PsaF (*42*).

Growth of Mutants. Figure 3 shows the results of growth tests of wild-type, the PSI minus mutant PsaA:C575D, and the four tryptophan mutants under heterotrophic (acetate-containing solid medium) and phototrophic (minimal medium) conditions. All strains were capable of heterotrophic growth in both darkness and light (50 μeinstein m^{-2} s^{-1}) with the exception of the C575D mutant that displays the extreme light sensitivity typical of PSI-deficient mutants (*29*). On minimal medium in the presence of oxygen, both the W693H and W693L mutants fail to grow and the W702H and W702L mutants grow poorly. However, removal of the oxygen allows the phototrophic growth of all four mutants. This demonstrates that a functional PSI complex is present in each mutant but that the site-directed changes introduced into the PSI core result in increased oxygen sensitivity. This phenomenon was first reported by Fisher et al. (*35*) for site-directed changes in PsaC and may result from PSI-mediated reduction of oxygen to form free radical species.

Photoaccumulation of the Phyllosemiquinone and Resultant EPR Spectra. Figure 4 shows the EPR spectra photoaccumulated in wild-type and mutant *C. reinhardtii* digitonin PSI preparations at 205 K in the presence of dithionite. Short periods of photoaccumulation in the wild-type preparation at pH 8 (Figure 4a) produce a spectrum at $g = 2.0047$ and $\Delta H_{ptp} = 0.875$ mT as previously reported in preparations from *C. reinhardtii* (*39*), spinach (*36*), and *Anabaena variabilis* (*17*). However, the unresolved proton hyperfine splittings giving rise to the distinctive spectra reported in refs *36* and *17* are less apparent. The spectra presented in Figure 4a photoaccumulated at pH 8 have been normalized for chlorophyll concentration and confirm that all mutants are assembling the photosystem I reaction center. The signal intensity of the photoaccumulated phyllosemiquinone is not an accurate reflection of the total amount of phyllosemiquinone that can be photoaccumulated since photoaccumulation was carried out for varying periods in order to maximize phyllosemiquinone photoaccumulation and minimize chlorophyll anion photoaccumulation (Figure 4). The signal intensity of spectra do indicate that all mutants contain substantial amounts of phylloquinone that can be reduced by photoaccumulation.

Photoaccumulation of preparations at pH 10 and 205 K for short periods (Figure 4b) gives rise to spectra with unresolved proton hyperfine splittings that are more characteristic of the phyllosemiquinone spectra reported for other organisms (*36*, *17*). The WT and W702 mutants show characteristic semiquinone EPR spectra of $\Delta H_{ptp} = 0.875$ mT at both pH 8 and pH 10 (Figure 4a,b), but the spectrum photoaccumulated in W693L and W693H is significantly broader when photoaccumulation is carried out at pH 10 ($\Delta H_{ptp} \cong 1$mT), suggesting that significant amounts of the chlorophyll electron acceptor $A_o^{\bullet -}$ is being photoaccumulated in these samples.

Proton ENDOR Spectra of the Photoaccumulated Samples. Changes in the electronic structure of the photoaccumulated phyllosemiquinone that might affect its redox function are much more likely to be resolved in proton ENDOR spectra, which will resolve and determine individual proton hyperfine couplings (hfcs). We have previously reported (*39*) the ENDOR spectrum of photoaccumulated phyllosemiquinone in *C. reinhardtii* and shown that it is very similar to those obtained for phyllosemiquinone photoaccumulated in PSI from spinach and *Anabena variabilis* (*18*). We are able to separate phyllosemiquinone and chlorophyll anion ENDOR spectra by taking advantage of the different relaxation (and thus temperature and microwave power dependence) of the two species. Figure 5 presents the proton ENDOR spectra of phyllosemiquinone photoaccumulated at pH 8 and 205 K on wild-type and W693 mutants of *C. reinhardtii.* The ENDOR spectra of W702 mutants were identical to those obtained from wild-type *C. reinhardtii* and are not shown. Table 1 shows details of the hyperfine coupling constants and resonance assignments for these spectra. The spectra demonstrate unequivocally that we are photoaccumulating phyllosemiquinone in both wild-type and mutant *C. reinhardtii.* The proton ENDOR spectra of wild type *C. reinhardtii* are of better signal-to-noise than those previously reported (*39*) and show that there is a greater asymmetry in the hydrogen bonding to the carbonyl oxygens of phyllosemiquinone in *C. reinhardtii* than observed in spinach and *A. variabilis* (*18*) (see Discussion). In both the W693L and W693H mutants, the hfcs to the 2-methyl group protons of the phyllosemiquinone are reduced, and the hydrogen bond hfcs are altered. However, these are relatively small changes in the electronic structure of the phyllosemiquinone (see Discussion) and by themselves would not be considered

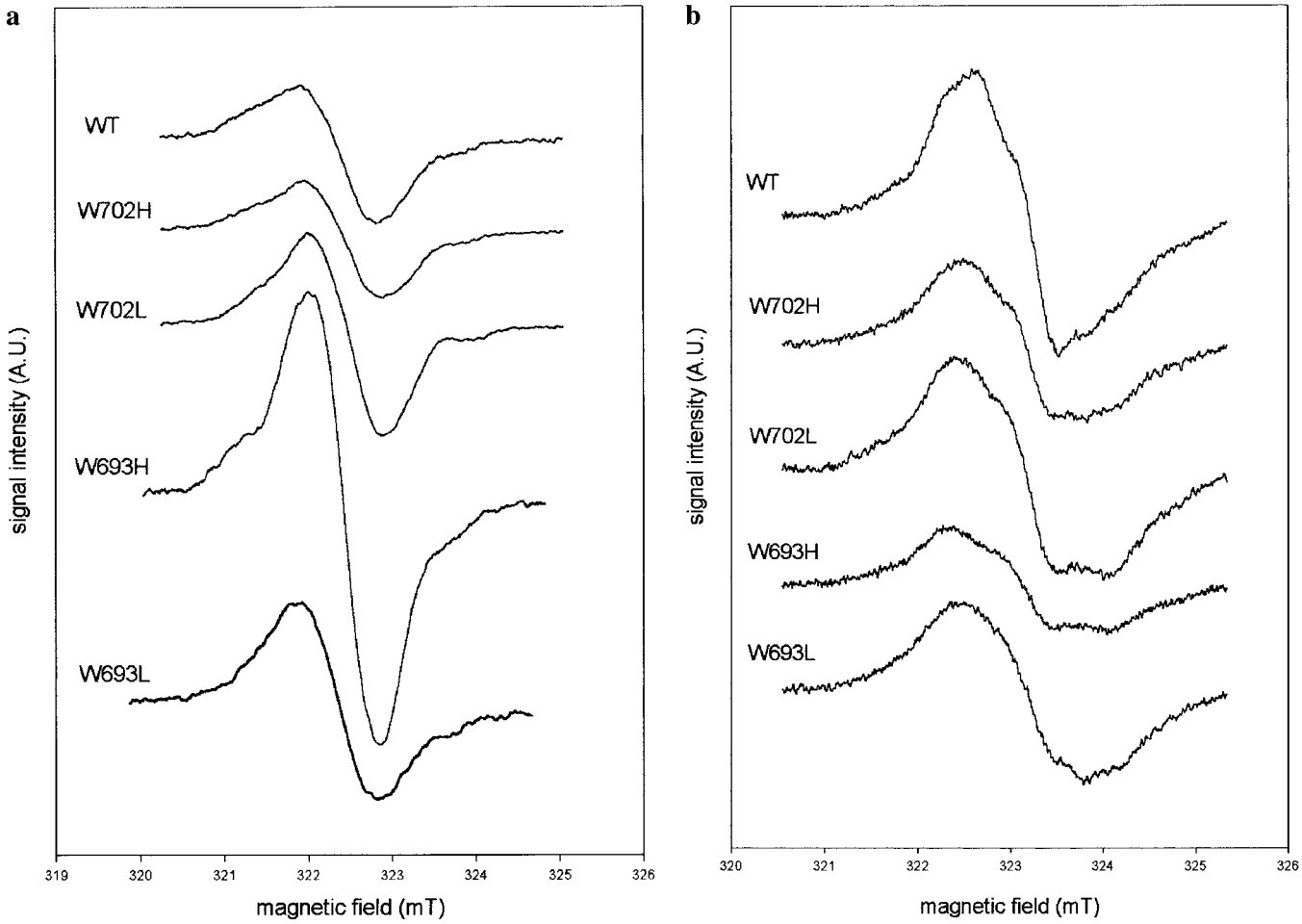

FIGURE 4: EPR spectra obtained by photoaccumulation at 205 K of digitonin PSI preparations from wild-type and mutant strains of *C. reinhardtii*. (a) The spectra obtained by photoaccumulation at pH 8 are normalized to a chlorophyll concentration of 2.15 mg of chlorophyll/mL. Samples were incubated at pH 8 as described in refs *36* and *17* and illuminated at 205 K for periods of between 30 s and 3 min to produce maximal phyllosemiquinone and minimal chlorophyll anion. EPR conditions are as follows: temperature, 70 K; microwave power, 40 μW; modulation amplitude, 0.2 mT. (b) The spectra obtained by photoaccumulation at pH 10 are not normalized and were obtained from samples with chlorophyll concentrations ranging from 2.5 to 5 mg/mL. The samples were illuminated at 205 K for periods ranging from 30 s to 2 min to produce maximal phyllosemiquinone and minimal chlorophyll anion. EPR conditions are as in panel a except the microwave power is 20 μW.

particularly significant. They do however indicate that the replacement of tryptophan by leucine/histidine on PsaA has altered the immediate environment of the photoaccumulated bound phyllosemiquinone.

Measurement of the Disappearance/Decay of the ESP ($P700^{\bullet+}/A_1^{\bullet-}$) Radical Pair Signal. We have measured the rate of decay of the ESP signal at 100 K, which reflects recombination between the radical pair $P700^{\bullet+}/A_1^{\bullet-}$. The rates are essentially unchanged between wild-type and mutant digitonin PSI preparations at around 20 $\pm$ 5 μs and are the same as those previously reported for *C. reinhardtii* (*39*) at these temperatures.

Measurement of the rate of disappearance of the ESP signal at 260 K should provide an estimate of the rate of forward electron transfer, and Figure 6 and Table 2 present the results of such measurements of wild-type and mutant digitonin PSI preparations. The rate of the forward reaction at room temperature has been found to be in the range of 200−300 ns in spinach by EPR and optical spectroscopic techniques (*12*−*14*). Schlodder et al (*38*) have shown that PSI forward electron transfer proceeds normally at temperatures down to 240 K, and the electron decays back to P700 from the iron−sulfur centers allowing repetitive flash averaging to be used, although the rate is temperature dependent. We have taken advantage of this to measure electron transfer from $A_1^{\bullet-}$ to F_x in preparations of *C. reinhardtii* at 260 K by monitoring the ESP signal. Control experiments with spinach photosystem I show that at 260 K the forward electron-transfer rate is 436 ns $\pm$ 127 as compared to 219 $\pm$ 92 at 293 K. The rate of forward electron transfer is similar in digitonin PSI preparations of wild-type and PsaA W702 mutants of *C. reinhardtii*, (Figure 6 and Table 2) to that in spinach. However, in the W693H and W693L mutants, the decay of the signal is much slower at around 1.3 μs.

This could be because either (a) the rate of forward electron transfer from $A_1^{\bullet-}$ to F_x has been slowed from ~400 ns to 1.3 μs or (b) the forward electron transfer from $A_1^{\bullet-}$ to F_x has been abolished since a rate similar to that observed in the W693H and W693L mutants was reported when F_x is removed (*12*) or when this FeS center was targeted by site-directed mutagenesis (*39*).

It might be argued that we are not measuring the true rate of electron transfer since forward electron transfer from $A_1^{\bullet-}$ to F_x has been slowed to a time domain where the loss of phase coherence between the radical pair giving rise to the

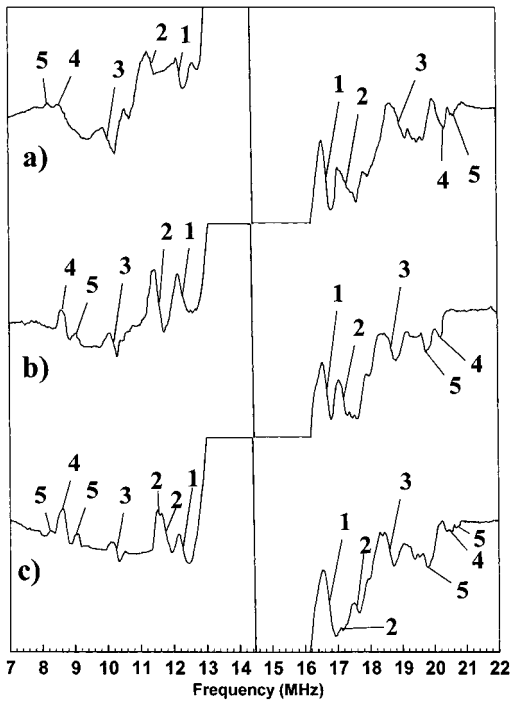

FIGURE 5: Proton ENDOR spectra of species photoaccumulated by illumination at 205 K of digitonin PSI preparations from (a) wild-type, (b) W693L, and (c) W693H mutant strains of *C. reinhardtii*. Samples were prepared at pH 8 and photoaccumulated as described in Materials and Methods at 205 K. ENDOR conditions were as follows: temperature, 70 K; microwave power, 3.0 mW; rf power, 100 W; rf modulation, 158 kHz.

Table 1: Hyperfine Coupling Constants (hfcs) and Assignments for $A_1^{\bullet-}$ Phyllosemiquinone Radicals in *C. reinhardtii*

	hfc (MHz)			
feature	WT	W693L	W693H	assignment
1	(−)4.5	(−)4.5	(−)4.5	H-bond $A_\perp$
2	(−)6.2	(−)5.5	(−)5.2 (−)6.0	H-bond $A_\perp$
3	8.9	8.5	8.3	methyl $A_\perp$
4	12.0	11.6	11.6	methyl $A_{\|\|}$
5	12.6	11.0	10.8 12.5	H-bond $A_{\|\|}$

ESP signal due to a T_2 relaxation process may become significant. Bock et al. (*46*) reported that an ESP signal arising from PSI had a lifetime that was microwave power dependent, which probably reflects an influence of T_2 on the measured lifetime. However it was the kinetics of decay of an ESP signal tentatively (and subsequently) (*12*, *13*) assigned to $P700^{\bullet+}$ F_x^- in the 600−700-ns range that was affected by microwave power and not the kinetics of decay of the ESP signal arising from the radical pair $P700^{\bullet+}/A_1^{\bullet-}$ in the 200−300-ns range. Although it may not be possible to unequivocally determine whether the change in rate of decay of the $P700^{\bullet+}/A_1^{\bullet-}$ signal observed reflects inhibition or slowing of forward electron transport, it clearly shows that the mutations at position PsaA693 significantly alter the environment of the quinone.

DISCUSSION

The results from Western blotting indicate that PSI is assembling properly in the mutants of *C. reinhardtii* (Figure 2) and that the minor polypeptides PsaF and PsaD are

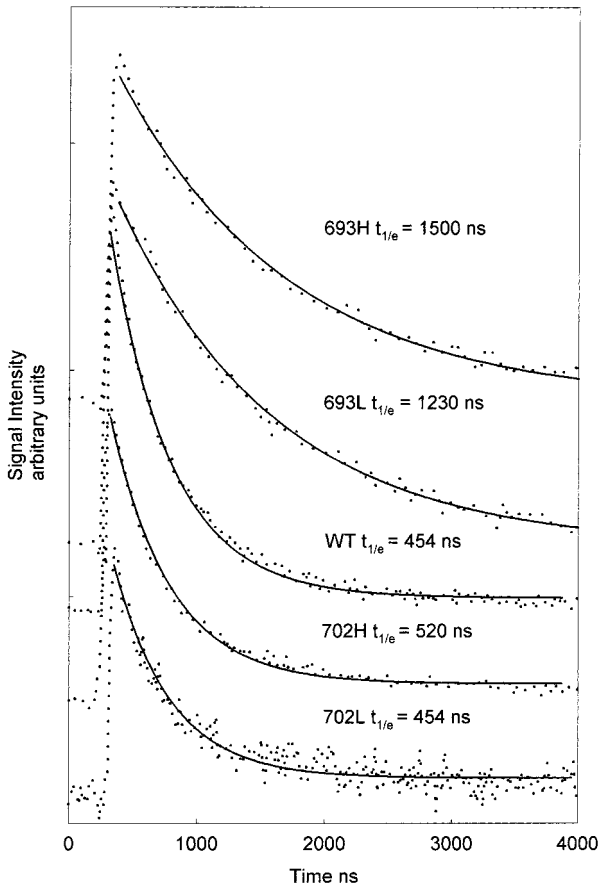

FIGURE 6: Pulsed EPR kinetics were measured at 260 K as described previously (*12*, *39*) using a Bruker ESP380 X-band spectrometer with a variable Q dielectric resonator (Bruker model 1052 DLQ-H 8907) fitted with an Oxford Instruments CF935 cryostat cooled with liquid nitrogen. Actinic illumination was supplied by a Nd:YAG laser (Spectra Physics DCR-11) with 10-ns pulse duration. Traces are examples of single experiments, with the results from a number of data sets shown in Table 2. Single-exponential fits are shown as a solid line.

Table 2: Rate of Disappearance of Electron Spin-Polarized (ESP) Signal Arising from the Radical Pair $P700^{\bullet-}/A_1^{\bullet-}$ at 260 K in Digitonin PSI Preparations from Wild-Type and Mutants of *C. reinhardtii*

sample	temp (K)	decay of spin polarized signal $t_{1/e}$ (ns)	no.of data sets
WT	260	355 ± 136	20
W702H	260	499 ± 48	5
W702L	260	478 ± 30	4
W693H	260	1340 ± 217	9
W693L	260	1365 ± 114	6

present. Although the results of spot test of the growth of mutants of W693 under phototrophic conditions in the presence of oxygen suggest that PSI is not functional in these mutants (Figure 3), growth of the mutants phototrophically in the absence of oxygen indicate that in fact PSI is functional in all of the mutants. Photoaccumulation of the phyllosemiquinone $A_1^{\bullet-}$ to obtain its EPR spectrum in preparations from *C. reinhardtii* requires careful characterization of the photoaccumulation conditions. We observe that photoaccumulation at any temperature above 205 K leads to photoaccumulation of a chlorophyll anion simultaneously with the photoaccumulation of the phyllosemiquinone, whereas in preparations from *Synechocystis* the phyllosemiquinone can

be cleanly photoaccumulated at 220 K (*23*). Photoaccumulation at 205 K for relatively short periods (up to 3 min) leads to photoaccumulation of the phyllosemiquinone in wild-type *C. reinhardtii*, although if carried out at pH 8 the spectrum lacks the characteristic line shape (Figure 4a) attributed to unresolved proton hfcs (*17*). The reasons for this are unclear, particularly since the proton ENDOR spectra demonstrate that a phyllsemiquinone is being photoaccumulated (Figure 5), and photoaccumulation at the same temperature but with samples at pH 10 leads to the characteristic line shape (Figure 4b) and identical proton ENDOR spectra (data not shown). The EPR spectra photoaccumulated in the PsaA W702 mutants are essentially identical to those seen in wild type, suggesting that these substitutions have had no effect on the binding or function of the photoaccumulated phyllosemiquinone. However, the EPR spectrum photoaccumulated in the PsaA W693L mutant suggest that less phyllosemiquinone is photoaccumulated, as the spectrum is broader (around 1 mT ΔH_{ptp}) and suggest that a chlorophyll anion is also being photoaccumulated. We are able to separate the proton ENDOR spectra of phyllosemiquinone and chlorophyll anions taking advantage of their different saturation characteristics. The spectra obtained and shown in Figure 5 and Table 1 confirm that phyllosemiquinone is being photoaccumulated. While the W702 mutants show no change in the electronic structure and thus local protein environment of the phyllosemiquinone, both the W693H and W693L mutants show small but discernible differences in the electronic structure of the photoaccumulated phyllosemiquinone $A_1^{\bullet-}$.

The wild-type spectrum shows the large 2-methyl hfcs observed for the same radical in *A. variabilis* and spinach (*18*). These are actually slightly smaller at $A_\perp = 8.9$ and $A_{||} = 12.0$ MHz as compared to $A_\perp = 9.0$ and $A_{||} = 12.6$ MHz in spinach, but these latter values were determined using Special TRIPLE and the difference is not really significant. It may be explained by the difference in the hydrogen bonding in *C. reinhardtii* below. This gives an unpaired electron spin density of 0.123 at C(*2*) (*43*).

The hydrogen bonding to $A_1^{\bullet-}$ in WT *C. reinhardtii* has a greater asymmetry than that to the same radical in *A. variabilis* and spinach (*18*). The hydrogen bond $A_\perp$ components being −4.5 and −6.2 MHz as compared to −5.0 and −5.8 MHz in *A. variabilis* and −5.2 and −6.0 MHz in spinach (only the perpendicular components are compared here since overlap prevents the clear assignment of all the hydrogen bond parallel components in the $A_1^{\bullet-}$ spectrum). In fact, the asymmetry is closer to that of *Heliobacterium chlorum* (*44*) (−5.0 and −6.5 MHz) but with longer O-H distances. These distances can be calculated, using the oxygen unpaired electron π spin density for phylloquinone in vitro (*20*) of 0.2, as 1.36 and 1.52 A. This provides further indication that there are two hydrogen bonds to the carbonyl oxygens of the phyllosemiquinone that is photoaccumulated, and the simplest interpretation is that the two carbonyl oxygens each have a hydrogen bond, particularly since the spin density found at the C2 (methyl protons) and C3 (β-CH_2 protons) positions in *A. variabilis* and spinach (*18*) is very similar.

In both the W693L and W693H mutants, the hfcs to the 2-methyl group are reduced to $A_\perp = 8.5/A_{||} = 11.6$ MHz and $A_\perp = 8.3/A_{||} = 11.6$ MHz, respectively (Figure 5 and Table 1). Since the unpaired electron spin density is proportional to A_{iso}, this represents reduction of spin density at C(*2*) of 4.1% to 0.118 and 5.7% to 0.116, respectively. Neither of these is particularly significant, but the unusually large 2-methyl hfc previously reported for $A_1^{\bullet-}$ (*18*) has been associated with the low E_M of this electron acceptor. Therefore, any changes in this hfc may be associated with changes in the A_1 binding site, which enables A_1 to function in forward electron transfer.

The hydrogen bond hfcs are also altered in the mutants. In both mutants the weaker hydrogen bond ($A_\perp = -4.5$ MHz) is maintained while the O-H distance is increased in the other hydrogen bond. In the W693L mutant, the hydrogen bond hfc is decreased to −5.5 MHz, which corresponds to an increase in O-H distance from 1.36 to 1.42 A. In the W693H mutant, the situation is complicated by apparent heterogeneity since there seem to be three hydrogen bond hfcs. One is the weaker hydrogen bond visible in WT ($A_\perp = -4.5$ MHz), another is very similar to the strong hydrogen bond in WT ($A_\perp = -6.0$ MHz), while there is a third apparent hydrogen bond hfc with $A_\perp = -5.2$ MHz corresponding to an O-H distance of 1.45 A. All these changes are too small to be detected in X-ray crystal structures but, since they give rise to shifts of over 1 MHz in the spectrum, are relatively straightforward to measure using ENDOR. That only one of the two H-bond hfcs is affected by the mutations suggests that they give rise to a specific structural change and not to generalized damage of the A_1 binding site. Although the W693H mutant gives rise to two different new H-bond hfcs, these are discrete values of the H-bond hfc, suggesting two different structures and not random disorganization. Therefore, overall the ENDOR data show that the W693 mutants give rise to specific changes in the A_1 binding site that correlate with those properties of the quinone that are implicated in controlling forward electron transfer.

It is interesting to speculate that the heterogeneity in the W693H mutants may arise from the relatively low pK_a of the histidine ring, which could cause it to be in two different protonation states at the experimental pH, whereas the pK_a of the tryptophan N(1)H is very high (∼12); therefore, such protonation state heterogeneity should not arise (given the usual caveats about extrapolating pK_a values from simple compounds to proteins).

It is difficult to resolve any features in the proton ENDOR spectra of WT or mutant *C. reinhardtii* that might correspond to the β-CH_2 protons at C(*3*) because of the hydrogen bond feature with $A_\perp = -4.5$ MHz, which is the stronger feature and obscures those of the β-CH_2 protons (Figure 5).

Although the changes in the electronic structure of the photoaccumulated phyllosemiquinone in the mutant strains are not particularly large, they do indicate that substitution of histidine/leucine for the PsaA W693 tryptophan has led to changes in the protein binding of the phyllosemiquinone. We had expected that substitution of histidine for tryptophan would maintain binding of the phylloquinone but had expected that substitution of a relatively bulky leucine might displace the phylloquinone by steric hindrance. This is evidently not the case in all the PSI assembled, as phyllosemiquinone is contributing to the photoaccumulated EPR spectra of W693L shown in Figure 4 and the proton ENDOR spectra of the photoaccumulated signal in this mutant conclusively identify a phyllosemiquinone (Figure 5 and

Table 1). When the ability of the phylloquinone to transfer electrons forward to F_x is monitored by looking at the rate of disappearance of the ESP signal, a dramatic effect of mutants of PsaA W693 is observed (Figure 6 and Table 2). Instead of the ~400-ns rate associated with forward electron transfer from a phyllosemiquinone to F_x in *C. reinhardtii* at 260 K (*12*, *39*), a rate of ~1300 ns is observed. So it seems that the rate of forward electron transfer is reduced (or perhaps even abolished) when the tryptophan is substituted by either histidine or leucine, which supports the hypothesis that tryptophan may assist in poising the redox potential of the phylloquinone/phyllosemiquinone redox couple so that it is able to transfer electrons to F_x (*20*, *22*). It has been suggested by analogy with the reaction center of purple photosynthetic non-sulfur bacteria that PsaB is the active branch of electron transfer (*26*), since the electron spin density in $P700^{\bullet+}$ is almost exclusively on the PsaB chlorophyll. However, here we are having a profound effect on electron transfer forward from the phyllosemiquinone by substitution of a residue on PsaA. This suggests strongly that the forward electron transfer from phyllosemiquinone to F_x monitored by the rate of disappearance of the ESP signal is occurring on the PsaA branch of cofactors. It is interesting in this context to note that a recent publication (*45*) analyzed quinone binding motifs in proteins and concluded that motifs were identifiable for the Q_A and Q_B ubiquinone binding pockets in the reaction centers of purple photosynthetic bacteria. Similar motifs were identified in the PsaB (Q_A type motif) and PsaA (Q_B type motif) core proteins of the PSI heterodimer.

Recently Joliot and Joliot suggested that possibly both branches of electron transfer (PsaA and PsaB branches) were active in PSI (*27*). They observed two phases of phyllosemiquinone reoxidation as monitored by absorbance changes in a mutant of *Chlorella sorokiniana* with half-times of ~18 and ~160 ns. This in their view could be explained by one of two hypotheses. Either PSI reaction centers are present in two conformational states that differ in the reoxidation rate of the phyllosemiquinone or alternatively the two phylloquinones corresponding to the two branches of the PSI heterodimer are both involved in electron transfer. If you accept the second hypothesis, it could then explain the observations reported above. The "fast" phase of electron transfer would not be detected by the pulsed EPR methods we use that have an effective resolution of ~50 ns. We are then only observing the "slow" branch of electron transfer, which is inactivated by the W693H/L transformations and may well be located on the PsaA branch of the PSI heterodimer. Since there is less than a factor of 10 difference between the rates of electron transfer in the two branches proposed, some electron transfer would always occur on the PsaA branch. If the ESP technique is monitoring the "slow" branch of electron transfer, then the phyllosemiquinone that is photoaccumulated at 205 K is probably also that involved in this "slow" branch of electron transfer, since the two techniques are monitoring a phyllosemiquinone with the same electronic structure. In a recent publication (*42*), Golbeck and co-workers concluded that only one branch of electron transfer is functional in PSI reaction centers since inhibition of the photoaccumulation of one phyllosemiquinone by deletion of PsaE and PsaF did not result in photoaccumulation of a second phyllosemiquinone. However, we have previously reported (*36*) that it is possible to photoaccumulate the second phyllosemiquinone, although it requires more extreme conditions than those employed here to photoaccumulate the first phyllosemiquinone.

Experiments to construct mutants of the PsaB polypeptide are in progress and should hopefully clarify whether both the PsaB and PsaA branches are active in forward electron transfer. The improvements anticipated in the resolution of the PSI structure should provide further insight into the environment around the phylloquinones and will guide future mutagenesis studies aimed at understanding the mechanism of electron transfer in PSI

ACKNOWLEDGMENT

We acknowledge the contribution of Dr. E. Hamacher to preliminary experiments on photoaccumulation of phyllosemiquinone. We thank J.-D. Rochaix (University of Geneva), D. Bryant (Pennsylvania State University), and K. Redding (University of Alabama) for the gift of antibodies and Professors P. R. Rich and J. H. A. Nugent for helpful discussions on quinone-binding sites.

REFERENCES

1. Brettel, K. (1997) *Biochim. Biophys. Acta 1318*, 322−373.
2. Webber, A. N., and Bingham, S. E. (1998) in *The Molecular Biology of Chloroplasts and Mitochondria in Chlamydomonas* (Rochaix, J.-D., Goldschmidt-Clermont, M., Merchant, S., Eds.) pp 325−348, Kluwer Academic Publishers, Dordrecht, The Netherlands.
3. Fish, L. E., Kuck, U., and Bogorad, L. (1985) *J. Biol. Chem. 260*, 1413−1421.
4. Schubert, W. D., Klukas, O., Krauss, N., Saenger, W., Fromme, P., and Witt, H. T. (1997) *J. Mol. Biol. 272*, 741−769.
5. Schoeder, H.-U., and Lockau, W. (1986) *FEBS Lett. 199*, 23−27.
6. Klukas, O., Schubert, W. D., Jordan, P., Krauss, N., Fromme, P., Witt, H. T., and Saenger, W. (1999) *J. Biol. Chem. 274*, 7361−7367.
7. Biggins, J., and Mathis, P. (1988) *Biochemistry 27*, 1494−1500.
8. Höj, P. B., and Møller, B. L. (1986) *J. Biol. Chem. 261*, 14292−14300.
9. Wynn, R. M., and Malkin, R. (1988*) FEBS Lett. 229*, 293−297.
10. Li, N., Zhao, J. D., Warren, P. V., Warden, J. T., Bryant, D. A., and Golbeck, J. H. (1991) *Biochemistry 30*, 7863−7872.
11. Yu, L., Zhao, J. D., Muhlenhoff, U., Bryant, D. A., and Golbeck, J. H. (1993*) Plant Physiol. 103*, 171−180.
12. Moenne-Loccoz, P., Heathcote, P., MacLachlan, D. J., Berry, M. C., Davis, I. H., and Evans, M. C. W. (1994) *Biochemistry 33*,10037−10042.
13. Van der Est, A., Bock, C., Golbeck, J., Brettel, K., Setif, P., and Stehlik, D. (1994) *Biochemistry 33*, 11789−11797.
14. Luneberg, J., Fromme, P., Jekow, P., and Schlodder, E. (1994) *FEBS Lett. 203*, 225−229.
15. Fujita, I., Davis, M. S., and Fajer, J. D. (1978) *J. Am. Chem. Soc. 100*, 6280.
16. Chamarovsky, S. K., and Cammack, R. (1982) *Photobiophys 4*, 195−200.
17. Heathcote, P., Moenne-Loccoz, P., Rigby, S. E. J., and Evans, M. C. W. (1996) *Biochemistry 35*, 6644−6650.
18. Rigby, S. E. J., Evans, M. C. W., and Heathcote, P. (1996) *Biochemistry 35*, 6651−6656.
19. MacMillan, F. (1996) Ph.D. Thesis, Freie Universitat, Berlin.
20. Hanley, J. A., Deligiannakis, Y., MacMillan, F., Bottin, H., and Rutherford, A. W. (1997) *Biochemistry 36*, 11543−11549.
21. Van der Est, A., Prisner, T., Bittl, R., Fromme, P., Lubitz, W., Mobius, K., Stehlik, D. (1997) *J. Phys. Chem. B 101*, 1437.

22. Kamlowski, A., Altenberg-Greulich, B., Van der Est, A., Zech, S. G., Bittl, R., Fromme, P., Lubitz, W., and Stehlik, D. (1998) *J. Phys. Chem. B 102*, 8278−8287.
23. McMillan, F., Hanley, J. A., van der Weerd, L., Knupling, M., Sun, Un., and Rutherford, A. W. (1997) *Biochemistry 36*, 9297−9303.
24. Zech, S. G., Van der Est, A., and Bittl, R. (1997) *Biochemistry 36*, 9774−9779.
25. Deligiannakis, Y., Hanley, J. A., and Rutherford, A. W. (1998) *Biochemistry 37*, 3329−3336.
26. Webber, A. N., Su, H., Bingham, S. E., Kass, H., Krabben, L., Kuhn, M., Jordan, R., Schlodder, E., and Lubitz, W. (1996) *Biochemistry 35*, 12857−12863.
27. Joliot, P., and Joliot, A. (1999) *Biochemistry 38*, 11130−11136.
28. Hallahan, B. J., Purton, S., Ivison, A., Wright, D., and Evans, M. C. W. (1995) *Photosynth. Res. 46*, 257−264.
29. Harris, E. H. (1989) *The Chlamydomonas Sourcebook. A Comprehensive Guide to Biology and Laboratory Use*, Academic Press, San Diego.
30. Goldschmidt-Clermont, M. (1991) *Nucleic Acids Res. 19*, 4083−4089.
31. Rochaix, J.-D., Mayfield, S., Goldschmidt-Clermont, M., and Erickson, J. (1988) Molecular biology of *Chlamydomonas*. In *Plant molecular biology: a practical approach* (Shaw, C. H., Ed.) IRL Press, Oxford.
32. Farah, J., Rappaport, F., Choquet, Y., Joliot, P., Rochaix, J.-D. (1995) *EMBO J. 14*, 4976−4984.
33. Diner, B. A., and Wollman, F. A. (1980) *Eur. J. Biochem. 110*, 521−526.
34. Boardman, N. K. (1970) *Methods Enzymol. 23*, 268−276.
35. Fisher. N., Sétif, P., and Rochaix, J.-D. (1997) *Biochemistry 36*, 93−102.
36. Heathcote, P., Hanley J. A., and Evans, M. C. W. (1993) *Biochim. Biophys. Acta 1144*, 54−61.
37. Thurnauer, M. C., and Norris, J. R. (1980) *Chem. Phys. Lett. 76*, 557−561.
38. Schlodder, E., Flakenberg, K., Gergeleit, M., and Brettel, K. (1998) *Biochemistry 37*, 9466−9476.
39. Evans, M. C. W., Purton, S., Patel, V., Wright, D., Heathcote, P., and Rigby, S. E. J. (1999). *Photosynth. Res. 61*, 33−42.
40. Rigby, S. E. J., Nugent, J. H. A., and O'Malley, P. J. (1994) *Biochemistry 33*, 1734−1742.
41. Rigby, S. E. J., Nugent, J. H. A., and O'Malley, P. J. (1994) *Biochemistry 33*, 10043−10050.
42. Yang, F., Shen, G. Z., Schluchter, W. M., Zybailov, B. L., Ganago, A. O., Vassiliev, I. R., Bryant, D. A., and Golbeck, J. H. (1998) *J. Phys. Chem. B. 102*, 8288−8299.
43. McConnell, H. M. (1956) *J. Chem. Phys. 24*, 764.
44. Muhiuddin, I. P., Rigby, S. E. J., Evans, M. C. W., Amesz, J., and Heathcote, P. (1999) *Biochemistry 38*, 7159−7167.
45. Fisher, N., and Rich, P. R. (2000) *J. Mol. Biol. 296*, 1153−1162.
46. Bock, C. H., van der Est, A. J., Brettel, K., and Stehlik, D. (1989) *FEBS Lett. 247*, 91−96.

BI0019489